Applied Geochemistry 89 (2018) 49–58

Contents lists available at ScienceDirect

Applied Geochemistry

journal homepage: www.elsevier.com/locate/apgeochem

# Origin of calcium sulfate-type water in the Triassic carbonate thermal water system in Chongqing, China: A chemical and isotopic reconnaissance

Qiong Xiao[a,b], Yongjun Jiang[b,*], Licheng Shen[b], Daoxian Yuan[a,b]

[a] Key Laboratory of Karst Dynamics, MLR & Guangxi, Institute of Karst Geology, Chinese Academy of Geological Sciences, Guilin 541004, China
[b] Chongqing Key Laboratory of Karst Environment & School of Geographical Sciences, Southwest University, Chongqing 400715, China

ARTICLE INFO

Editorial handling by Dr. I. Cartwright

*Keywords:*
Geothermal system
Stable isotopes
Hydrogeochemistry
Triassic carbonate reservoir
Chongqing
China

ABSTRACT

Chongqing, located in the southwestern China, was named as "A spa city of the world". It's most geothermal reservoirs are developed in carbonate rock aquifers, and those thermal waters are characterized by high concentrations of sulfate and low $HCO_3^-$. However, little was known about the origin and genesis of those thermal waters, which is necessary for their protection and determination of regime of exploitation. Therefore, thermal and surface waters were sampled seasonally and analyzed for hydrogeochemical and isotopic compositions ($\delta^{18}O/\delta^{2}H$; $\delta^{34}S–SO_4$; $\delta^{18}O–SO_4$) to decipher the origin of the thermal waters in the Triassic carbonate aquifers in Chongqing area. Key questions include the relative significance of hydrothermal processes and solute supply. The results showed that: (1) the major chemical composition of analyzed the thermal waters from Chongqing area was characterized by Ca-$SO_4$; (2) the $\delta^{2}H$ and $\delta^{18}O$ values of the thermal waters ranged from −48.6‰ to −63.1‰ with an average value of −54.2‰, and from −6.5‰ to −9.2‰ with an average value of −8.0‰, respectively, indicating that the thermal waters originated from the local rain water with an elevation of 415 m to 1453 m above mean sea level; (3) the estimated geothermal temperatures varied from 63.8 °C to 78.3 °C (Quartz), indicating that the depth of the geothermal reservoir varied from 411 m to 1728 m, which is located in the Lower Triassic Jialingjiang formation; (4) the $\delta^{34}S\text{-}SO_4^{2-}$ and $\delta^{18}O\text{-}SO_4^{2-}$ in the geothermal waters ranged from 29.7‰ to 34.1‰ with a mean value of 32.1‰, and from 12.5‰ to 16.5‰ with a mean value of 15.2‰, respectively, suggesting that the high $SO_4^{2-}$ concentrations resulted mainly from the dissolution of gypsum in the second part of the Lower Triassic Jialingjiang Formation; (5) three processes of water-rock interactions (gypsum dissolution, carbonate dissolution by carbonic acid and carbonate dissolution by sulfuric acid) in the thermal system were unveiled by the hydrogeochemical and isotopic models. Among these three processes, gypsum dissolution seems to be primarily responsible for solute composition of the thermal water. This study also indicates the integration of hydrogeochemical and isotopic data is very useful tool to decipher the origin and genesis of the carbonate thermal waters.

## 1. Introduction

The carbonate thermal waters, which are characterized by Ca-sulfate, have been well known because they are used for curative purpose since the Middle Ages in the world (Boschetti et al., 2005; Capecchiacci et al., 2015). Meanwhile, the large changes of $\delta^{34}S$ in carbonate-associated sulfate (CAS) in limestones over geological time have been found (Claypool et al., 1980; Kah et al., 2001, 2004; Bottrell and Newton, 2006), especially at the Permian–Triassic boundary. The extreme changes of $\delta^{34}S$ occurring over very short geological time scales have long attracted special interest in the global sulfur cycle.

Chongqing City, the only municipality in southwestern China, holds rich shallow geothermal resources, which are mostly distributed in the core area of a series of eastern Sichuan parallel anticline developed in the Triassic-Jurassic strata. Because the exploitation of the shallow geothermal resources is mainly for the spa leisure tourism, Chongqing was named as "A spa city of China" in 2011 and "A spa city of the world" in 2012. Some studies have been focused on the geochemical characteristics of the thermal waters (Cao, 2007; Yang et al., 2017), and results indicated that most thermal waters are found from the carbonate aquifers and show very high concentrations of $SO_4^{2-}$ (more than 1000 mg/l) and low $HCO_3^-$ values (less than 200 mg/l) in Chongqing area, which are very similar to other Triassic carbonate thermal waters in the world (Boschetti et al., 2005; Capecchiacci et al., 2015). Nevertheless, little was known about the origin and genesis of thermal waters, especially on the dominant sources of sulfur of thermal waters in Chongqing area, which is necessary for their protection and determination of regime of exploitation.

* Corresponding author.
*E-mail addresses:* xiaoqiong-8423@163.com (Q. Xiao), jiangjyj@swu.edu.cn (Y. Jiang).

https://doi.org/10.1016/j.apgeochem.2017.11.011
Received 6 June 2017; Received in revised form 19 November 2017; Accepted 23 November 2017
Available online 26 November 2017
0883-2927/ 

A wide range of approaches are used to study the origin and genesis of thermal waters, including the applications of structural, hydraulic, hydrogeochemical and isotopic methods, and the investigation of fluid inclusions (González et al., 2000; Rissmann et al., 2015). Sulfate is a ubiquitous component in thermal waters, and is derived from a variety of sources such as precipitation and oxidation of sulfide minerals in the strata and dissolution of sulfate evaporates. Because of large S isotope variation exists in Earth's rocks (~80–100‰) with small S isotope fractionations (~1–2‰) during the oxidation/dissolution of S-bearing minerals (Clark and Fritz, 1997; Szynkiewicz et al., 2015), the $\delta^{34}S\text{-}SO_4$ can precisely pinpoint major sources of S participating in water-rock interaction. Thus, in the past decades, $\delta^{34}S\text{-}SO_4^{2-}$ has been widely used to trace the sources of sulfate in geothermal waters (Ohmoto, 1986; Martinez, 1993; Jennifer et al., 2000; Kusakabe et al., 2000; Çelmen and Çelik, 2009; Fatma et al., 2011; Peters et al., 2011; Risacher et al., 2011; Dupalová et al., 2012; Loges et al., 2012; McDermott et al., 2015; Rissmann et al., 2015), and formation characteristics of gypsiferous units (Orti et al., 2002; Palmer et al., 2004; Çelmen, 2008). Meanwhile, some geothermal waters originated form the carbonates have been studied such as the hot springs in Hungary (Dublyansky, 1995) and in Italy (Boschetti et al., 2005; Capecchiacci et al., 2015) and the thermal power stations in Kazakhstan and Germany (Keller, 1991; Berge and Veal, 2005), and results indicated that the origin and genesis of the thermal waters from carbonates are more complex than those from other thermal reservoirs.

Thus, seasonal variations in the concentrations of dissolved $SO_4^{2-}$ and their isotopic compositions coupled with hydrochemical parameters, and $\delta^2H$ and $\delta^{18}O$ of the thermal and surface waters were used to determine the origin of the thermal waters, and discuss the potential $SO_4^{2-}$ sources of the thermal waters derived from the carbonates in Chongqing area. The purpose of this study is that hydrogeochemical and isotopic data were integrated to decipher the origin of the carbonate thermal waters and trace quantitatively the sources of the solute compositions in these thermal waters. Three processes of water-rock interactions (gypsum dissolution, carbonate dissolution by carbonic acid and carbonate dissolution by sulfuric acid) in the carbonate thermal system were quantitatively unveiled by the hydrogeochemical and isotopic models, respectively. The results indicate that the gypsum dissolution rather than the carbonate dissolution by carbonic acid or sulfuric acid is the dominant control process for the solute compositions of the thermal waters in the study area.

## 2. Outline of study area

Chongqing municipality is located in the eastern Sichuan Basin, southwest China (Fig. 1), the transitional area between the Qinghai-Tibet

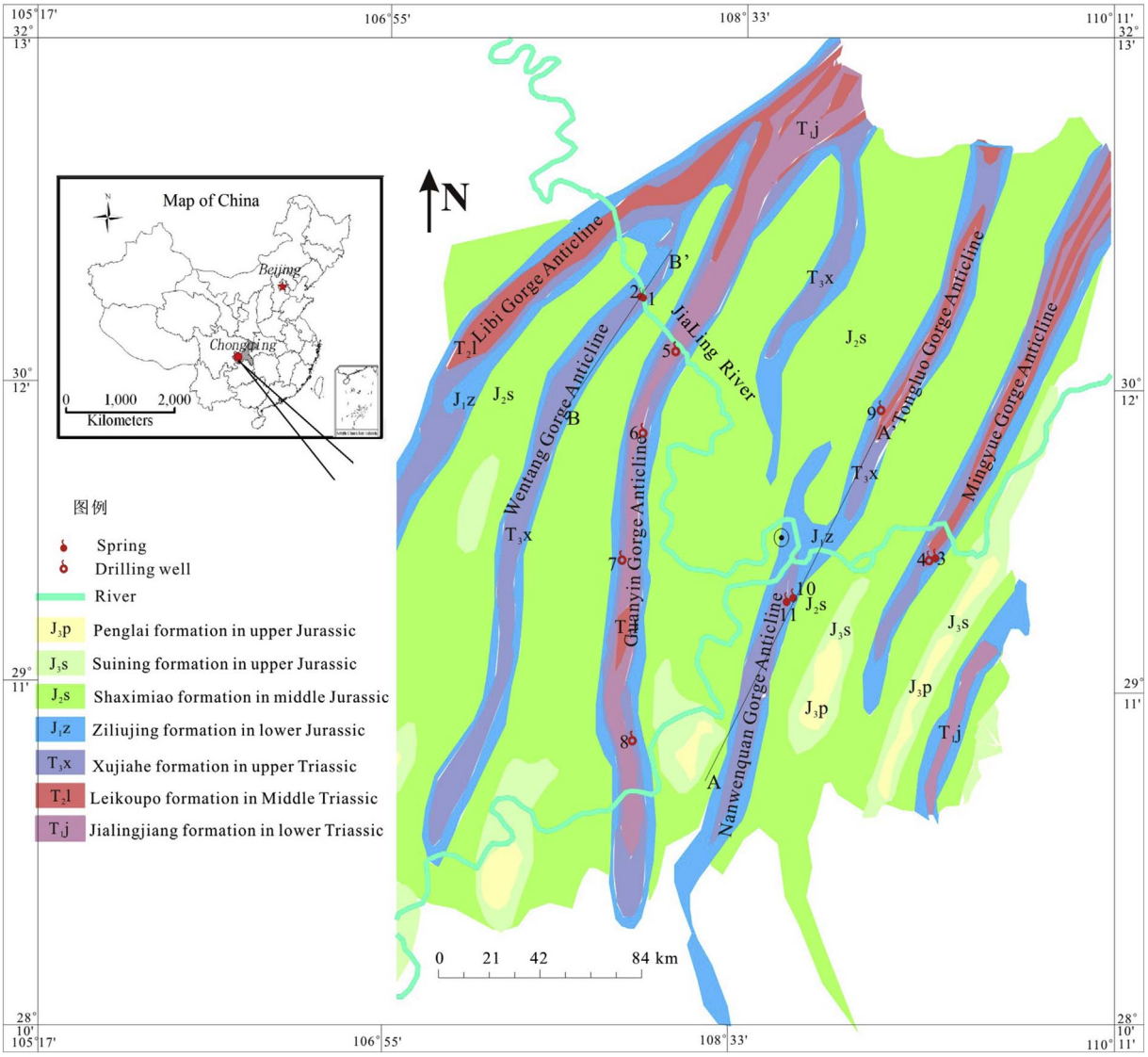


**Fig. 1.** Location, hydrogeological map and distribution of thermal water samples in Chongqing.

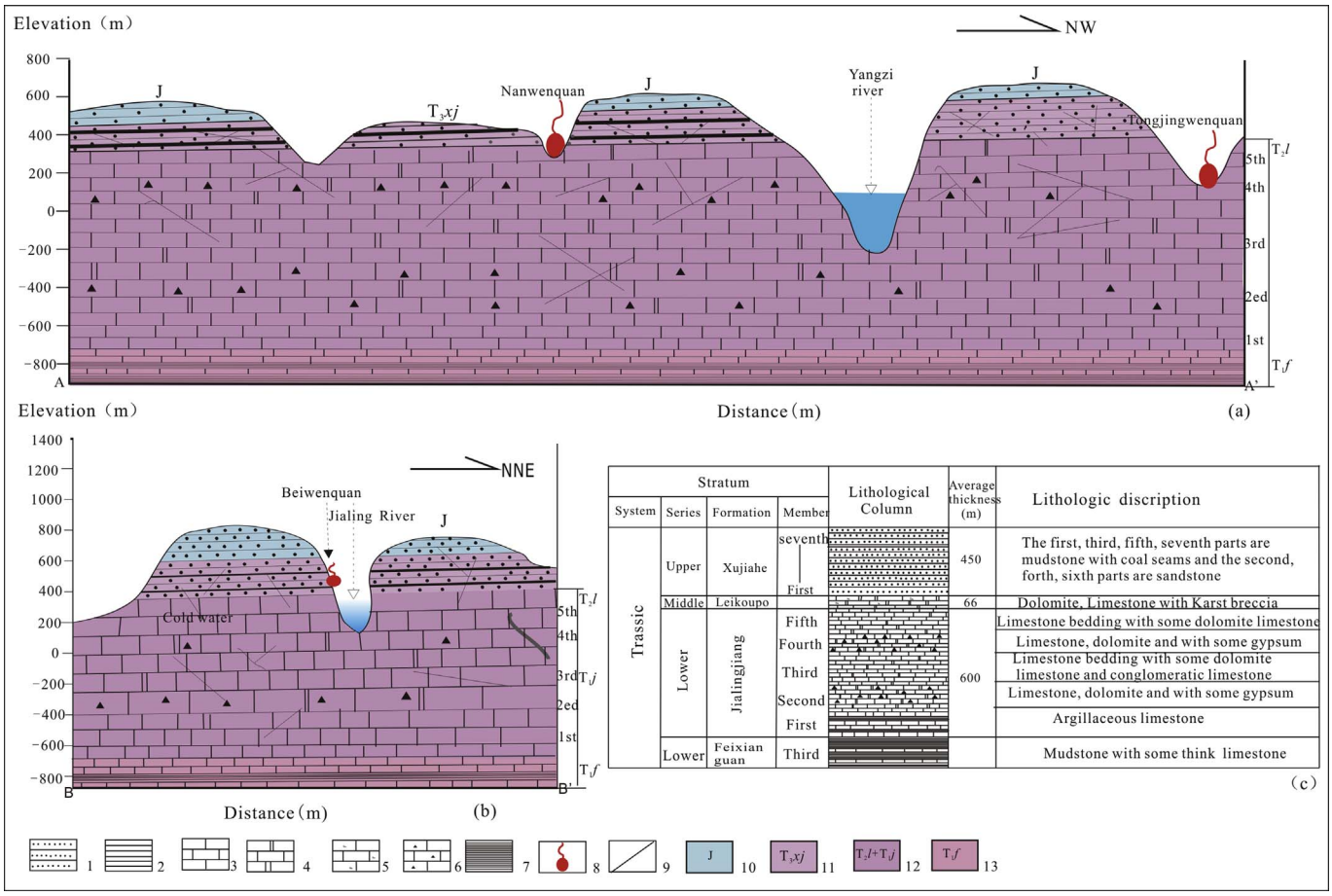


**Fig. 2.** Cross section of the Geological units and thermal springs.
1. Sandstone 2. Shale 3. Limestone 4. Dolomitic limestone 5. Dolomitic limestone with karst breccia 6. Dolomitic limestone with gypsum. 7. Mudstone. 8. hot spring. 9. fissures. 10. Jurassic. 11. Xujiahe formation in upper Triassic. 12. Leikopo formation in middle Triassic and Jialingjiang formation in lower Triassic. 13. Feixianguan formation in lower Triassic. (a): Nanwenquan gorge anticline and Tongluo gorge anticline, Yangtze River cross this region and develop a deep-cutting gorge which breaks down the static hydraulic connection in neighbouring anticlines. (b): Wentang gorge anticline, The Jialingjiang River cross this region and develop a deep-cutting gorge which breaks down the static hydraulic connection in neighbouring anticlines. (c): the host rock lithofacies division of study area.

Plateau and the middle and lower reaches of the Yangtze River plain. Its geographical coordinate is 105°17′–110°11′E, 28°10′–32°13′N, covering an area of about 8.24 × $10^4$ $km^2$, of which carbonate rocks covering about 3.0 × $10^4$ $km^2$ or 36.5% of the total area. The elevation of Chongqing province is between 75 and 2800 m with a mean elevation of 400 m above average sea level. The climate is primarily subtropical monsoonal with a mean annual precipitation of 1200 mm and a mean air temperature of 17 °C. The monsoonal climate results in a rainy season from April to September and a dry season from October to March next year.

Total volume of thermal water is about one billion cubic meters in the downtown and suburb of Chongqing metropolitan area (Liu, 2005), which belongs to the fold bundle in the eastern of Sichuan, the sub-first grade geotectonic unit-Sichuan Basin. The basic structure is made up of a series of line shape pectination folds or box folds that are NE—NNE trending approximate parallel and dissymmetry. Most of the fractures are high-angle SE-NWW trending thrust faults. The Jialingjiang River and Yangtze River cross this region and develop a deep-cutting gorge which breaks down the static hydraulic connection in neighbouring anticlines (Fig. 1). Most thermal waters were exposed from the anticlinal axis, where the outcrops are carbonate rocks of the Lower Triassic Jialingjiang Formation ($T_1j$) with the thickness of about 510-1060 m (average thickness of about 600 m), and include five parts, of which the first and third part are limestone bedding with some dolomite limestone and conglomeratic limestone, and the second and the forth part are limestone, dolomite and some gypsum (Sichuan Geological Bureau, 1991). The anticlinal wings are carbonate rocks with some gypsum of the Middle Triassic Leikoupo Formation ($T_2l$) with an average thickness of 66 m, which overlie the Jialingjiang Group, and sandstones of the Upper Triassic Xujiahe Formation ($T_3xj$), which is hundreds to thousands meters thick and with an average of 450 m, and was divided into 7 parts, of which the first, third, fifth and seventh parts are mudstone with some coal seams, and the second, fourth and sixth parts are sandstone (Gao et al., 2009), which served as thermal-protective coating (Fig. 2). The cataclastic rocks mingled with carbonate of the Lower Triassic Feixianguan Formation ($T_1$f) underlain the Jialingjiang Group and serve as a wonderful water barrier. Thus, the carbonate rocks of anticlinal axis (the Lower Triassic Jialingjiang Formation) are comprised of the groundwater aquifer, and sandstones of the anticlinal wings (the Upper Triassic Xujiahe Formation) with higher elevation are the recharge area, and the Lower Triassic Feixianguan Formation underlain the Jialingjiang Group serves as the aquitard.

## 3. Materials and methods

A total of 30 thermal springs samples from 12 representative springs, of which four natural springs and eight drilling wells i.e. Beiwenquan (BWQ), Shuiwenzhan (SWZ), Liugongqiao (LGQ), Qingmuguanwenquan (QMGWQ) in Wentang gorge anticline, Yishangwenquan (YS), Tianciwenquan (TC), Feicuihu (FCH), Nanhaiwenquan (NH) in Guanyin gorge anticline, Nanwenquan (NWQ and NWQ2), Tongjingwenquan (TJ) in Tongluoxia gorge anticline and Dongquanredong (DQRD), Dongquanbayi (DQBY) in Mingyue gorge

**Table 1**
Basic message of the sampling sites.

| Sampling sites | Natural spring or drilling well | Structure | Exposed strata | Aquifer lithology | Exploitation | Discharge ($m^3$/d) |
|---|---|---|---|---|---|---|
| Beiwenquan (BWQ) | Natural spring | Wentang gorge anticline | $T_3xj$ | limestone | Spa | > 2213 |
| Shuiwenzhan (SWZ) | Natural spring | Wentang gorge anticline | $T_3xj$ | limestone | Spa | > 2233 |
| Cengjiang (CJ) | Drilling well | Wentang gorge anticline | $T_1j$ | limestone | Public Swimming Pool | 1123 |
| Yishangwenquan (YS) | Drilling well | Guanyin gorge anticline | $T_1j$ | limestone | Spa | 1342 |
| Feicuihu (FCH) | Drilling well | Guanyin gorge anticline | $T_1j$ | limestone | Community swimming pool | 834 |
| Nanhaiwenquan (NH) | Drilling well | Guanyin gorge anticline | $T_1j$ | limestone | Spa | 823 |
| Tianciwenquan (TC) | Drilling well | Guanyin gorge anticline | $T_1j$ | limestone | Spa | 2389 |
| Nanwenquan (NWQ) | Natural spring | Nanwenquan gorge anticline | $T_1j$ | limestone | Spa | 1198 |
| Tongjingwenquan (TJ) | Drilling well | Tongluo gorge anticline | $T_1j$ | limestone | Spa | 2143 |
| Nanwenquan 2(NWQ2) | Natural spring | Nanwenquan gorge anticline | $T_1j$ | limestone | Undeveloped use | 512 |
| Dongquanbayi (DQBY) | Drilling well | Mingyue gorge anticline | $T_1j$ | limestone | Public Swimming Pool | 520 |
| Dongquanredong (DQRD) | Drilling well | Mingyue gorge anticline | $T_1j$ | limestone | Undeveloped use | – |

anticline, were collected in January (winter dry season) and July (summer rainy season) of 2009, and April (spring season) and October (autumn season) of 2010, respectively (Fig. 1 and Table 1). Additional 5 surface waters (Jianglingjiang River) were collected.

Hand-held measurements of field parameters, including water temperature (T), pH, dissolved oxygen (DO) and electrical conductivity (EC), were taken during each sampling trip in situ, using HQ340d water quality multimeter (HACH, America), with resolutions of 0.1 °C, 0.1 mg/l, 1 μS/cm, respectively. $Ca^{2+}$ and $HCO_3^-$ were determined by a test kit with a titration pipette (Aquamerck) in the field with resolutions of 2 mg/l and 0.1 mmol/l, respectively.

Water samples for ion analyses were collected by injection syringes and were immediately filtered into pre-rinsed plastic containers through 0.45 μm filter membranes. $NO_3^-$ and $SO_4^{2-}$ were determined by the ultraviolet–visible spectrometry, and $Cl^-$ was analyzed by titration of silver nitrate. Resolutions of all anion analysis were 0.01 mg/l. Nitric acid was added to samples which were collected in 100 ml plastic containers to be acidified until pH < 2.0 for major cation analysis ($K^+$, $Na^+$, $SiO_2$ and $Mg^{2+}$) by an inductively coupled plasma optimal emission of spectrometry (ICP-OES) with resolutions of 0.01 mg/l at the Chongqing Key Laboratory of Karst Environment.

The samples for $\delta^{34}S\text{-}SO_4^{2-}$ and $\delta^{18}O\text{-}SO_4^{2-}$ analysis were collected in 500 ml plastic bottles and acidified with 5 ml 1:1 HCl and 5 drops of $HgCl_2$. Sulfate-S isotope was measured from the dissolved $SO_4^{2-}$. After adding a 10% $BaCl_2$ solution, dissolved $SO_4^{2-}$ was recovered by $BaSO_4$ precipitation. The precipitate was collected on a 0.45 mm Millipore membrane filter and dried. The $\delta^{34}S\text{-}SO_4^{2-}$ and $\delta^{18}O\text{-}SO_4^{2-}$ isotope composition was determined by an Elemental Analyzer (Carlo Erba 1108) coupled with an IRMS (Delta C Finningan Mat 251). Notation is expressed in terms of δ (‰) relative to the Vienna Canyon Diablo Troilite (V-CDT) standard. The isotope ratios were calculated using international and laboratory standards. The reproducibility of samples calculated from standards systematically interspersed in the analytical batches was ± 0.2‰ and ± 0.5‰ for $\delta^{34}S\text{-}SO_4^{2-}$ and $\delta^{18}O\text{-}SO_4^{2-}$, respectively. The isotope analyses were conducted at Wuhan Institute of Geology and Mineral Resources (China).

The $\delta^2H$ and $\delta^{18}O$ isotopic ratios of water samples were analyzed by high-precision laser spectroscopy (LWIA-24d, Los Gatos Research, USA) at Key Laboratory of Karst Dynamics, MLR & Guangxi, Institute of Karst Geology, Chinese Academy of Geological Sciences. All the hydrogen and oxygen isotope values are expressed in permil (‰) deviations relative to Vienna Standard Mean Ocean Water (V-SMOW). The overall analytical errors are 0.8‰ and 0.25‰ for $\delta^2H$ and $\delta^{18}O$, respectively. Analytical results were shown in Table 1S (Supporting Material).

## 4. Results

### 4.1. Hydrochemical characteristics of thermal waters

As shown in Table 1S and Fig. 3, the hydrogeochemistry of the thermal waters were characterized by high concentrations of $Ca^{2+}$, $Mg^{2+}$ and $SO_4^{2-}$ and low concentrations of $HCO_3^-$. The obvious spatial and seasonal variations of hydrogeochemistry of the thermal waters were observed.

The thermal waters were neutral to alkaline, with pH values from 6.7 to 8.0 (average 7.3), and showed lower values in summer and autumn than in spring and winter. Temperature of the thermal waters varied from 28.5 °C to 53.5 °C with a mean value of 39.7 °C, and showed higher values in summer and spring than in autumn and winter. The EC values ranged between 2390 and 3400 μS/cm with a mean value of 2801 μS/cm, and higher values were observed in summer and winter. The DO (Dissolved oxygen) values ranged between 0.0 and 0.3 mg/l with a mean value of 0.1 mg/l. $Ca^{2+}$ was the most abundant cation, varying from 514 to 729 mg/l with a mean of 606 mg/l, and showed higher concentrations in the winter and autumn and lower concentrations in the summer and spring, followed by $Mg^{2+}$, varying from 104 to 149 mg/l with a mean of 124 mg/l, and showed higher concentrations in the winter. $SO_4^{2-}$ was the most common anion, varying from 1340 to 1941 mg/l with a mean of 1575 mg/l, and showed higher concentrations in the spring and summer, followed by $HCO_3^-$, varying from 152 to 231.8 mg/l with a mean of 180.8 mg/l and also showed higher concentrations in the spring and summer. $Ca^{2+}$ and $SO_4^{2-}$ were accounted for 90% of the cations and anions, respectively. As shown in

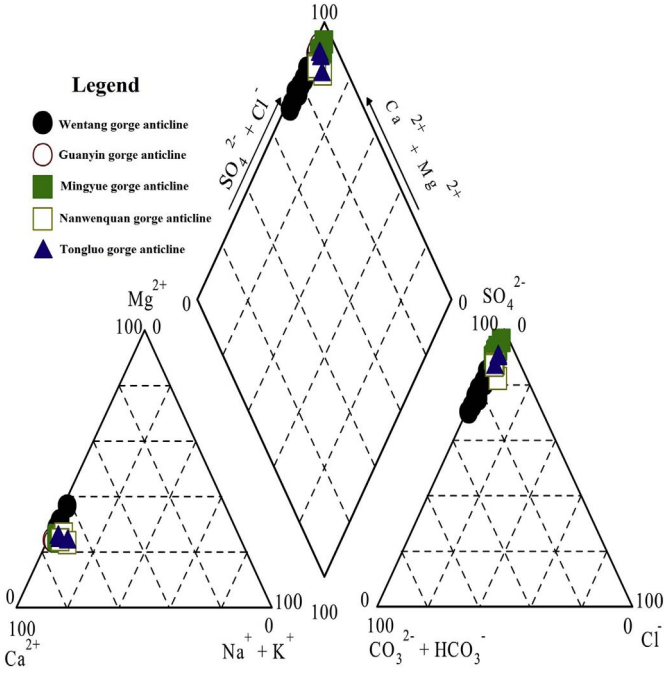


**Fig. 3.** Piper diagram for the thermal waters.

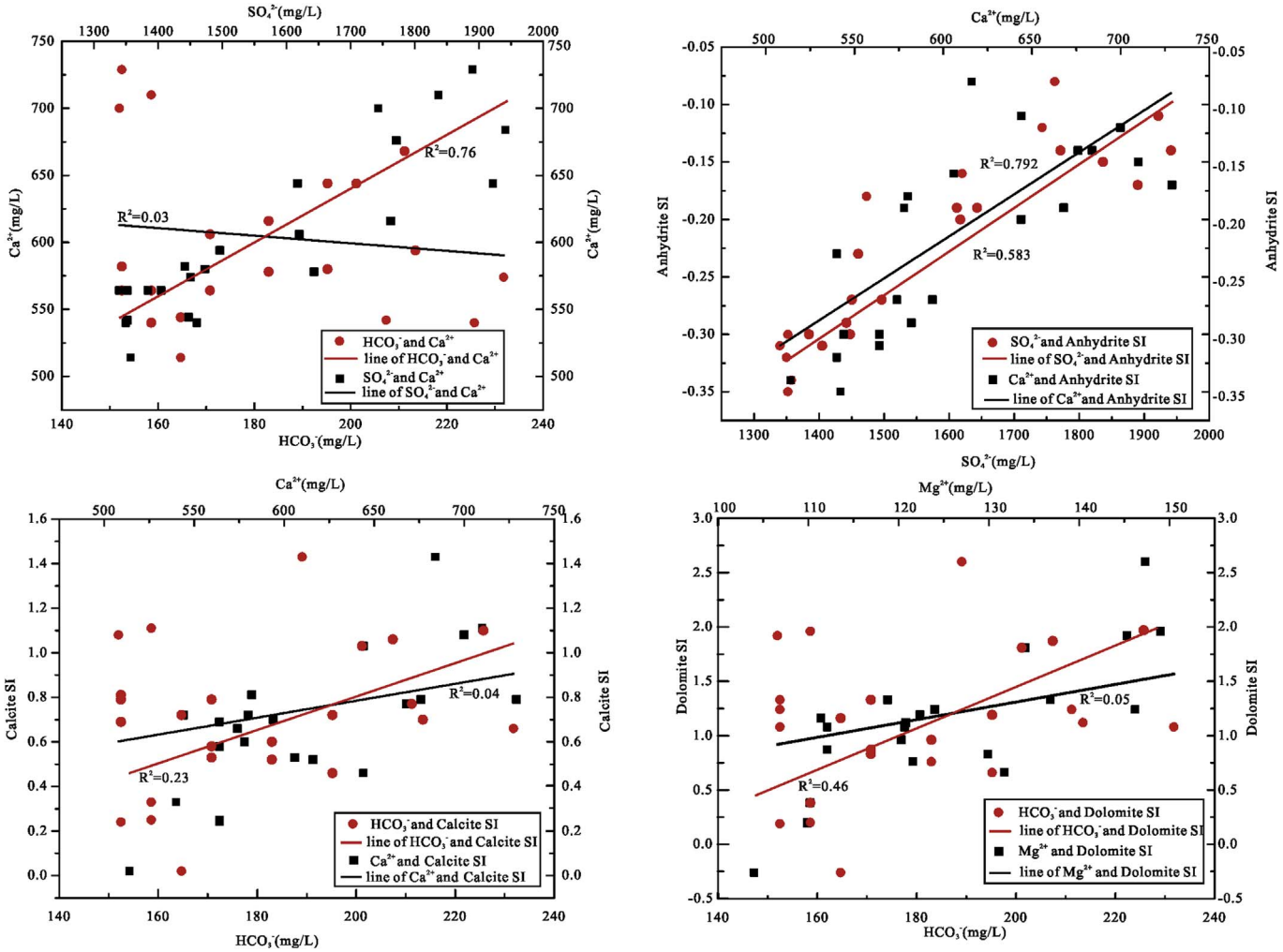


**Fig. 4.** Relationships between major ions and saturation indexes.

Fig. 3, the hydrochemical facies of all the thermal waters were characterized by Ca-$SO_4$ type.

In contrast, the surface waters from Jialingjiang River showed much lower concentrations of $Ca^{2+}$ (an order of magnitude lower, 52–70 mg/l), $Mg^{2+}$ (an order of magnitude lower, 8.9–16.7 mg/l) and $SO_4^{2-}$ (2.5 order of magnitude lower, 29.6–38.9 mg/l) than those in the thermal waters, and the $HCO_3^-$ concentrations are similar, with values of about 170 mg/l. The chemistry type of the surface water was Ca-$HCO_3$.

Water-rock interaction is the major factor controlling the groundwater chemistry. As shown in Fig. 4a, high linear correlation between $SO_4^{2-}$ and $Ca^{2+}$ concentrations ($R^2$ = 0.76) was observed throughout the observation period, suggesting that the main water-rock interaction is evaporate dissolution. However, there is no correlation ($R^2$ = 0.03) between $Ca^{2+}$ and $HCO_3^-$, which implies that carbonate weathering was not the main source of $Ca^{2+}$ in the thermal aquifer. The Anhydrite SI (SIa), Calcite SI (SIc) and Dolomite SI (SId) were calculated by PHREEQC and the results were shown in Fig. 4 (b, c, d). The SIa was from −0.35 to 0.05, which is nearly saturated state. High linear correlations between $SO_4^{2-}$ and SIa ($R^2$ = 0.583), and $Ca^{2+}$ and SIa ($R^2$ = 0.792) were observed, suggesting that $Ca^{2+}$ and $SO_4^{2-}$ were derived from the evaporate dissolution. The SIc and SId varied from 0 to 1.4 and −0.3 to 2.5, respectively. Low linear correlations between $Ca^{2+}$ and SIc ($R^2$ = 0.04), $HCO_3^-$ and SIc ($R^2$ = 0.23), $Mg^{2+}$ and SId ($R^2$ = 0.005), and $HCO_3^-$ and SId ($R^2$ = 0.46) were observed, indicating that carbonate weathering was not the main source of $Ca^{2+}$, $Mg^{2+}$ and $HCO_3^-$ in the thermal waters.

### 4.2. $\delta^2H$-$H_2O$ and $\delta^{18}O$-$H_2O$

As shown in Table 1S, the $\delta^2H$ and $\delta^{18}O$ values of the thermal waters ranged from −48.6‰ to −63.1‰ with an average value of −54.2‰, and from −6.5‰ to −9.2‰ with an average value of −8.0‰, respectively, and showed subtle seasonal variations with lower values in summer (−55.5‰ and −8.4‰, respectively). The values of $\delta^2H$ and $\delta^{18}O$ of the surface water of JLJ river were wide distributed (−51.9‰ to −73.84‰, −9.99‰ to −7.4‰, respectively), and the values of $\delta^{18}O$ of the surface waters in Qingmuguan area were about −6.63‰ (Wang, 1991).

### 4.3. Isotopes of dissolved $SO_4^{2-}$

The $\delta^{34}S$-$SO_4^{2-}$ and $\delta^{18}O$-$SO_4^{2-}$ of the thermal waters varied from 29.7‰ to 34.1‰ with a mean value of 32.1‰ and from 12.5‰ to 16.5‰ with a mean value of 15.2‰, respectively, and showed obvious seasonal variations with lower values in summer. The surface water showed much lower $\delta^{34}S$-$SO_4^{2-}$ and $\delta^{18}O$-$SO_4^{2-}$, having mean values of 16.3‰ and 4.8‰, respectively.

## 5. Discussion

### 5.1. Source of thermal waters

Hydrogen and oxygen isotopes can be used to trace the circulation of waters and are also applied to trace the origin of the thermal water

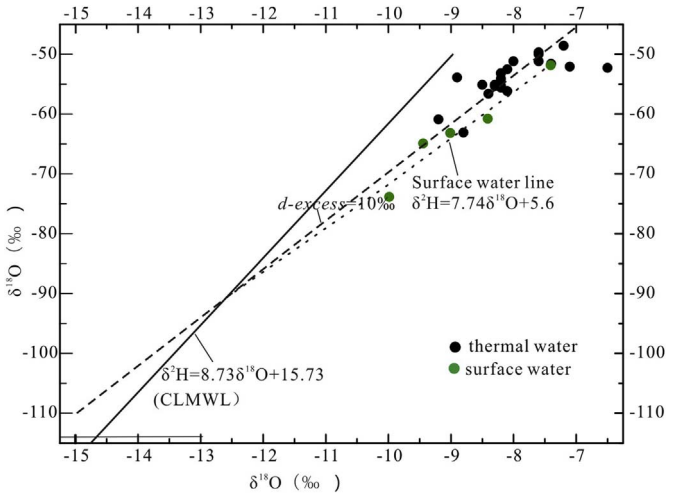


**Fig. 5.** $\delta^2H$ -$\delta^{18}O$ plot of the thermal and surface waters from Chongqing.

(Chandrajith et al., 2013; Yang et al., 2017). According the relationships between the $\delta^2H$-$\delta^{18}O$ of the thermal waters and $\delta^2H$-$\delta^{18}O$ of local meteoric waters, the origin of the thermal waters can be determined. Li et al. (2010) had given the Chongqing Local Meteoric Water Line (CLMWL):

$$\delta^2H = 8.73\ \delta^{18}O + 15.73\ r^2 = 0.97 \quad (1)$$

As shown in Fig. 5, all the data points are very close to the CMWL, indicating that local precipitation is the major origin of the thermal and surface waters.

The d-excess is defined as d-excess = $\delta^2H$-8$\delta^{18}O$, and can be used to explain the evaporation effect of the surface and thermal waters. When d-excess < 10‰, the waters would have evaporation effect (Juske et al., 2008). The average values of d-excess of thermal and surface waters are 10.3 and 7.3, respectively, indicating there is little evaporation effect for the thermal waters.

The hydrogen and oxygen isotopic compositions of precipitation have obvious altitude effect (Wang, 1991), and the recharge elevation can be calculated by the following equation:

$$H = \frac{R - (R1)}{\rho} * 100 + h \quad (2)$$

where H is the recharge elevation; *R* is the values of $\delta^{18}O$ of thermal waters; *R1* is the values of $\delta^{18}O$ of surface waters in Qingmuguan area; *h* is the altitude of the surface water; ρ is the oxygen isotopic gradient value of precipitation. As demonstrated in the literature (Wang, 1991), the values of $\delta^{18}O$ (*R1*) and the altitude (h) of surface waters in Qingmuguan area are −6.63‰ and 465 m (Wang, 1991), respectively, and the oxygen isotopic gradient value of precipitation (ρ) is about −0.26‰/100 m in the eastern part of Tibet (Yu et al., 1980). Thus, the theoretical values of recharge elevation of the thermal waters can be obtained (Table 2). The calculated recharge elevation of the thermal waters varied from 415 to 1453 m with an average value of 1000 m above mean sea level.

### 5.2. Temperature and depth of the geothermal reservoir

The silica geothermometer is widely used to estimate subsurface temperatures in hot spring system (Fournier and Rowe, 1966). Meanwhile, no any secondary siliceous minerals were found in the rock from the drill core in the NWQ (Cao, 2007). Thus, the quartz geothermomerter can be calculated through the following equation (Fournier, 1977):

$$\text{Quartz T(°C)} = 1309/(5.19\text{-lg}C_S) - 273 \quad (3)$$

**Table 2**
Temperature and depth of the geothermal reservoir.

| Sites | TW | $SiO_2$ | QT | Depth |
|---|---|---|---|---|
| | °C | mg/l | °C | m |
| FCH | 53.5 | 20.1 | 63.8 | 411 |
| NH | 37.1 | 20.3 | 64.2 | 1082 |
| NWQ2 | 40.1 | 26.3 | 74.2 | 1364 |
| DQBY | 45.6 | 24.5 | 71.4 | 1032 |
| DQRD | 38.1 | 22.5 | 68.1 | 1199 |
| TJ | 47.7 | 22.3 | 67.7 | 801 |
| BWQ | 35.1 | 29.1 | 78.3 | 1728 |
| SWZ | 35.8 | 24.3 | 71.1 | 1411 |

where $C_S$ is the concentration of the $SiO_2$.

The calculated results were shown in Table 2. The estimated temperatures of the geothermal reservoir by Eq. (3) were between 63.8 °C and 78.3 °C. Thus, based on the average geothermal gradient, 2.5°C/100 m, in Sichuan basin (Nanjiang Hydrogeological & Engineering Geology Brigade, Geology and Mineral Resources Bureau of Investigation, Sichuan province, China. 1977), the estimated depth of the geothermal reservoir varied from 411 m to 1728 m (Table 2). Therefore, it can be concluded that the thermal reservoir is located in the Lower Triassic Jialingjiang formation.

### 5.3. Sources of the dissolved $SO_4^{2-}$

Dissolved $SO_4^{2-}$ in the geothermal waters can be originated from a multitude of sources, e.g., (1) sulfate deposition, (2) oxidation of sulfide minerals in the strata, and (3) dissolution of sulfate evaporates. As shown in Table 1S, surface waters cannot be major contributors of $SO_4^{2-}$ to the geothermal waters because the geothermal waters were more enriched in $SO_4^{2-}$ (average 1575 mg/l) than surface waters (average 32.0 mg/l) from the study area. As stated earlier, coal seams, located in the recharge area, are disseminated in the first; third, fifth and seventh stage of the Xujiahe Formation in the Upper Triassic and their presence could be a potential source of dissolved $SO_4^{2-}$ in the geothermal waters. Rich evaporate deposits (gypsum) found in the Jialingjiang Formation could be another important potential source of dissolved $SO_4^{2-}$ in the geothermal waters. As shown in Fig. 6 and Table 1S, obvious seasonal variations of $SO_4^{2-}$ concentrations, $\delta^{34}S$-$SO_4^{2-}$ and $\delta^{18}O$-$SO_4^{2-}$ were observed in the geothermal waters, indicating that there are complicated (multiple) S sources in the geothermal waters in different seasons. Therefore, dissolved $SO_4^{2-}$ in the geothermal waters could be originated mainly from the dissolution of sulfate evaporates and the oxidation of sulfide minerals in the strata of the study area.

As has been demonstrated by the literature, the $\delta^{34}S$-$SO_4^{2-}$ and $\delta^{18}O$-$SO_4^{2-}$ derived from the oxidation of sulfide minerals in the strata (coal) ranged from −6.1‰ to +7.4‰ with an average of −0.32‰ (Hong et al., 1992), and range from −5‰ to 4‰ (Krouse and Mayer, 2000), respectively. The $\delta^{34}S$-$SO_4^{2-}$ and $\delta^{18}O$-$SO_4^{2-}$ derived from the precipitation varied from −8.1‰ to −4.9‰(Hong et al., 1994), and from 8‰ to 15‰ (Li et al., 2013), respectively. Anomalously positive CAS-sulfur isotopes in Triassic have been observed all over the world, although the exact cause remains controversial (Claypool et al., 1980; Bottrell and Newton, 2006), e.g., the $\delta^{34}S$ of gypsum in Triassic varied from 25.1‰ to 27.6‰ in Germany (Clarke and Thode, 1964), and 28.2‰ and 28.3‰ in Utah, America (Claypool et al., 1980). In Sichuan Basin, China, the $\delta^{34}S$ of gypsum of Leikoupo Formation in the Middle Triassic ranged from +14.7‰ to +30.6‰ (Lin et al., 1998), and the $\delta^{34}S$ of gypsum of the fourth stage of Jialingjiang Formation in the Lower Triassic varied from +26‰ to +32‰ (Lin et al., 1998), and the $\delta^{34}S$ of gypsum of the second stage of Jialingjiang Formation in the Lower Triassic ranged from +32.5‰ to +36.2‰ (Lin et al., 1998). As

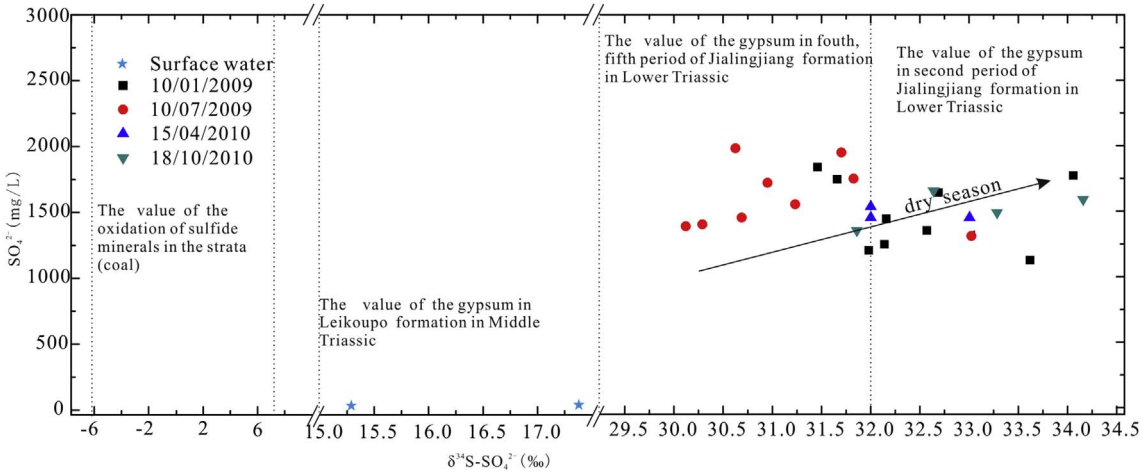


**Fig. 6.** Scatter plots of $\delta^{34}S\text{-}SO_4^{2-}$ vs. $SO_4^{2-}$ for water samples analyzed and potential S sources.

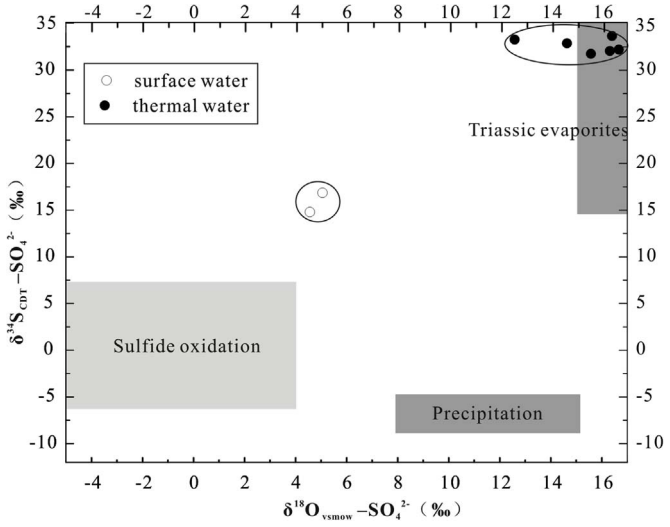


**Fig. 7.** Scatter plots of $\delta^{34}S\text{-}SO_4^{2-}$ vs. $\delta^{18}O\text{-}SO_4^{2-}$ for water samples analyzed and potential S sources.

shown in Figs. 6 and 7 and Table 1S, the sulfur isotopic values of dissolved $SO_4^{2-}$ in the thermal waters ranged from +32.0‰ to +33.1‰ with an average value of 32.4‰ in spring, from +29.7‰ to +33.1‰ with an average of +31.1‰ in summer, and from +31.8‰ to +34.1‰ with an average of 32.9‰ in autumn, and from +31.5‰ to +34.1‰ with an average of 32.6‰ in winter. The $\delta^{34}S\text{-}SO_4^{2-}$ values of the thermal waters in spring, autumn and winter (dry season) are very close to the $\delta^{34}S$ of gypsum of the second stage of Jialingjiang Formation, suggesting that the sulfate of the thermal waters in these seasons resulted mainly from the water-rock interaction in the second part of the Jialingjiang Formation, while the observed slight lower $\delta^{34}S\text{-}SO_4^{2-}$ of thermal waters in summer (rainy season) could be derived by a combination of the water-rock interaction in the second part of the Jialingjiang Formation and the oxidation of sulfide minerals in the Upper Triassic Xujiahe Formation. Meanwhile, The $\delta^{18}O\text{-}SO_4^{2-}$ in the thermal waters, ranging from 12.5‰ to 16.5‰, showed slight lower values than those in gypsum, varying from 14.5‰ to 32.5‰ (Li et al., 2011), and higher values than those in the surface and rain waters, supporting the hypothesis that indicating that the sulfate of the thermal waters could be derived by a combination of the dissolution of gypsum and the oxidation of sulfide minerals in the strata. Therefore, as indicated in Fig. 7, the $\delta^{34}S\text{-}SO_4^{2-}$ and $\delta^{18}O\text{-}SO_4^{2-}$ values in the thermal waters suggested that the sulfate of the thermal waters resulted mainly from the dissolution of gypsum in the second part of the Jialingjiang Formation in the Lower Triassic, a little from sulfide oxidation and precipitation.

### 5.4. Water-rock interaction: carbonate weathering vs. sulfate weathering

Another distinct hydrochemical feature of the thermal waters was the high concentrations of $SO_4^{2-}$ (more than 1000 mg/l) and low $HCO_3^-$ values (less than 200 mg/l), although the thermal waters were derived from the Triassic carbonate aquifers. As stated earlier, the second part of the Jialingjiang Formation in the Lower Triassic is made up of limestone and dolomite with some gypsum. Thus, the water-rock reactions are carbonate weathering and gypsum dissolution, which can be expressed as follows:

$$Ca_{(1-a)}Mg_aCO_3 + CO_2 + H_2O \rightarrow (1\text{-}a)Ca^{2+} + aMg^{2+} + 2HCO_3^- \quad (4)$$

$$CaSO_4 \rightarrow Ca^{2+} + SO_4^{2-} \quad (5)$$

Additionally, as indicated by the $\delta^{34}S\text{-}SO_4^{2-}$ of the thermal waters, $SO_4^{2-}$ partly resulted from the oxidation of sulfide minerals in the strata, and this process can be expressed as follow:

$$FeS_2 + H_2O + 7/2O_2 \rightarrow Fe^{2+} + SO_4^{2-} + 2H^+ \quad (6)$$

$$Ca_{(1-a)}Mg_aCO_3 + SO_4^{2-} + 2H^+ \rightarrow (1\text{-}a)Ca^{2+} + aMg^{2+} + H_2O + CO_2 + SO_4^{2-} \quad (7)$$

Thus, the thermal waters derived from different water-rock reactions will show different molar ratios of $(Ca^{2+}+Mg^{2+})/HCO_3^-$ and $(Ca^{2+}+Mg^{2+})/SO_4^{2-}$, of which the molar ratio between $(Ca^{2+}+Mg^{2+})$ and $HCO_3^-$ should be 0.5 based on Eq. (4), and the molar ratio between $Ca^{2+}$ and $SO_4^{2-}$ should be 1 based on Eq. (5), and based on Eq. (7), the molar ratio of $(Ca^{2+}+Mg^{2+})/SO_4^{2-}$ should be 1.

As shown in Table 1S, the molar ratios of $(Ca^{2+}+Mg^{2+})/HCO_3^-$ and $(Ca^{2+}+Mg^{2+})/SO_4^{2-}$ in the thermal waters ranged from 4.95 to 9.45 with a mean value of 6.98 (also may be caused by the instability of the $HCO_3^-$ under the conditions of heated and flowed), and from 1.14 to 1.34 with a mean value of 1.25, respectively, which deviated significantly from the expected molar ratios derived from Eq. (4) and Eq. (7), suggesting that the carbonate dissolution by carbonic or sulfuric acids could not the primary processes governing the solute compositions of $Ca^{2+}$, $Mg^{2+}$ and $SO_4^{2-}$ in the thermal waters. Also, as shown in Table 1S, the molar ratio of $Ca^{2+}/SO_4^{2-}$ in the thermal waters varied from 0.84 to 1 with a mean value of 0.93, although showed slight seasonal variations with lower values in summer (average 0.9), which were very closed to the expected the molar ratio between $Ca^{2+}$ and $SO_4^{2-}$ according to Eq. (5), suggesting the gypsum dissolution should be the primarily processes governing the solute compositions of $Ca^{2+}$ and $SO_4^{2-}$ in the thermal waters.

*5.4.1. Intensities discrimination of the water-rock interactions based on the hydrochemistry (model 1)*

According to Eq. (4), Eq. (5) and Eq. (7), we assumed that X, Y and Z mmol/l of carbonate dissolution by carbonic acid, gypsum dissolution and carbonate dissolution by sulfuric acid (oxidation of sulfide minerals), respectively, and the concentrations of $Ca^{2+}$, $Mg^{2+}$ and $SO_4^{2-}$ in the thermal waters can be calculated by following equations:

$$[Ca^{2+}] = (1\text{-}a)X + Y + (1\text{-}a)Z \quad (8)$$

$$[Mg^{2+}] = aX + aZ \quad (9)$$

$$[SO_4^{2-}] = Y + Z \quad (10)$$

where a is decided by the solubility of $CaCO_3$ and $MgCO_3$, which is 0.013 g/100 g and 0.43 g/100 g in 25 °C (Zhou et al., 1954), respectively. Thus, a is 13/430 in the study area.

The calculated results were shown in Table 2S. The contributions of carbonate dissolution by carbonic acid, gypsum dissolution and carbonate weathering by $H_2SO_4$ derived from the coal strata to total $Ca^{2+}$ in the thermal waters varied from 0.5% to 1.4% with a mean percentage of 0.8%, 98%–99% with a mean percentage of 98.6%, and 0%–0.8% with a mean percentage of 0.6%, respectively. The contributions of carbonate dissolution by carbonic acid and sulfuric acid derived from the coal strata to total $Mg^{2+}$ in the thermal waters varied from 27% to 98% with a mean percentage of 74.8%, and 2%–73% with a mean percentage of 25.2%, respectively. While the contributions of gypsum dissolution and carbonate weathering by sulfuric acid to total $SO_4^{2-}$ in the thermal waters varied from 79% to 100% with a mean percentage of 91.5%, and 0%–21% with a mean percentage of 8.5%, respectively. Therefore, based on the hydrochemical data, although there are different contribution of gypsum dissolution and carbonate weathering by carbonic and sulfuric acids to the solute compositions of the thermal waters in different seasons, it can be concluded that the gypsum dissolution rather than the carbonate dissolution by carbonic acid or sulfuric acid should be primarily responsible for the major solute compositions of the thermal waters (Ca-$SO_4$) in the study area.

*5.4.2. Intensities discrimination of the water-rock interactions based on the $\delta^{34}S$ (model 2)*

Stable isotope mixing models have become commonly applied tools in the environment sciences, and three - sources, two – isotopes mixing model have been applied to determine the three different of component (sulphides, evaporates and sulfate derived from precipitation) of S in groundwater using the $\delta^{34}S\text{-}SO_4^{2-}$ and the $\delta^{18}O\text{-}SO_4^{2-}$ measurement (Samborska et al., 2013). The system of equations in linear mixing model is written in the following form (Phillips and Gregg, 2001; Philips and koch, 2002).

$$\delta_T = f_A\delta_A + f_B\delta_B + f_C\delta_C \quad (11)$$

$$\lambda_T = f_A\lambda_A + f_B\lambda_B + f_C\lambda_C \quad (12)$$

$$1 = f_A + f_B + f_C \quad (13)$$

Where $f_A$, $f_B$ and $f_C$ are sulfur fractions from the sources A, B, and C in the mixture, $\delta_A$, $\delta_B$ and $\delta_C$ are the mean delta values of sulfur from the respective sources A, B and C, respectively. $\lambda_A$, $\lambda_B$ and $\lambda_C$ are the mean delta values of oxygen from respective sulfate sources, and $\delta_T$ and $\lambda_T$ are resulting delta values in the mixture.

In the thermal system, as shown in Table 1S, the geothermal waters were more enriched in $SO_4^{2-}$ (average 1575 mg/l) and also more enriched in the value of $\delta^{34}S\text{-}SO_4^{2-}$ (average is 32.1‰), subjoin that the dual-isotope approach ($\delta^{34}S\text{-}SO_4^{2-}$ and $\delta^{18}O\text{-}SO_4^{2-}$) defined most of the source of sulfate of the thermal water is Triassic evaporates, and then is from sulfide oxidation. So the model could be changed to two-sources, one–isotopes and to determine the two different of components (sulphides and evaporates) of S. The system of equation could be simplified as follow:

$$\delta_T = f_A\delta_A + f_B\delta_B \quad (14)$$

$$1 = f_A + f_B \quad (15)$$

As discussed in the previous section, dissolved $SO_4^{2-}$ in the geothermal waters was mainly from the dissolution of sulfate evaporates and the oxidation of sulfide minerals in the strata in the study area. Thus, given the $\delta^{34}S\text{-}SO_4^{2-}$ of gypsum from the Lower Triassic Jialingjiang Formation (mean value is +35.0‰) as $\delta_B$ and the oxidation of sulfide minerals from the Upper Triassic Xujiahe Formation (mean value is −0.32‰) as $\delta_A$, and the measured $\delta^{34}S\text{-}SO_4^{2-}$ in the geothermal waters as $\delta_T$, the contributions of gypsum dissolution and carbonate weathering by sulfuric acid to total $SO_4^{2-}$ in the thermal waters can be calculated by the following equation:

$$\delta^{34}S\text{-}SO_4^{2-}(\text{thermal water}) = 35.0‰ \times f_B - 0.32‰ \times (1\text{-}f_B) \quad (16)$$

where $f_B$ is percentage of $SO_4^{2-}$ derived from the gypsum dissolution of the second part of Jialingjiang Formation, and (1-$f_B$) is the percentage of $SO_4^{2-}$ derived from carbonate weathering by sulfuric acid. Also, the concentrations of $Ca^{2+}$ and $Mg^{2+}$ concentrations can be calculated out. The calculated results are shown in Table 2S.

As shown in Table 2S, The contributions of carbonate dissolution by carbonic acid, gypsum dissolution and carbonate weathering by $H_2SO_4$ derived from the coal strata to total $Ca^{2+}$ in the thermal waters varied from 0.5% to 0.8% with a mean percentage of 0.7%, and 98%–99% with a mean percentage of 99.0%, and 0%–0.8% with a mean percentage of 0.3%, respectively. The contributions of carbonate dissolution by carbonic acid and $H_2SO_4$ to total $Mg^{2+}$ in the thermal waters varied from 47% to 92% with a mean percentage of 76.1% and from 8% to 53% with a mean percentage of 23.9%, respectively. While the contributions of gypsum dissolution and $H_2SO_4$ to total $SO_4^{2-}$ in the thermal waters varied from 85% to 99% with a mean percentage of 91.1% and varied from 1% to 15% with a mean percentage of 8.9%, respectively.

As shown in Table 2S, the calculated concentrations of $Ca^{2+}$ were slight higher than the measured values in the thermal waters. This can be explained by that the deoxidation in the thermal systems, which the geothermal waters showed very low concentrations of DO (varying from 0 to 0.3 mg/l, Table 1S), was ignored in both of models. Sulfate reduction in the geothermal waters could be mediated by sulfate-reducing bacteria (SRB) under the condition of deoxidation and result in elevated the $\delta^{34}S\text{-}SO_4^{2-}$ and $\delta^{18}O\text{-}SO_4^{2-}$ in the geothermal waters (Rye et al., 1981; Bottrell et al., 2000; Spence et al., 2001; Gunn et al., 2006), and lead to the amount of sulfate and $Ca^{2+}$ derived from the carbonate dissolution by $H_2SO_4$ that comes from sulfide oxidation could be underestimated. Whatever, based on the $\delta^{34}S\text{-}SO_4^{2-}$ data, it can also be concluded that the gypsum dissolution rather than the carbonate dissolution by carbonic acid or sulfuric acid, should be primarily responsible for the solute compositions of the thermal waters in the study area. More important is that there are insignificant differences in the calculated results between the model 1 and model 2, suggesting that the integration of hydrogeochemical and isotopic data is very useful and valid to decipher the origin and processes governing the solute composition of the thermal waters.

*5.5. Conceptual model of formation and evolution of thermal waters*

Based on the discussions above, a conceptual model of formation and evolution of the thermal waters in Chongqing area can be established (Fig. 8). As shown in Fig. 8, surface waters originated from 460 m–1605 m elevation recharged the carbonate aquifers in the depth between 411 m and 1,728 m which comprise of some gypsum and sulfide minerals, and then discharged as natural hot springs along the karst fissures or conduits. The solute compositions of the thermal waters were primarily governed by the gypsum dissolution from the Lower Triassic Jialingjiang formation, partly by the carbonate dissolution by

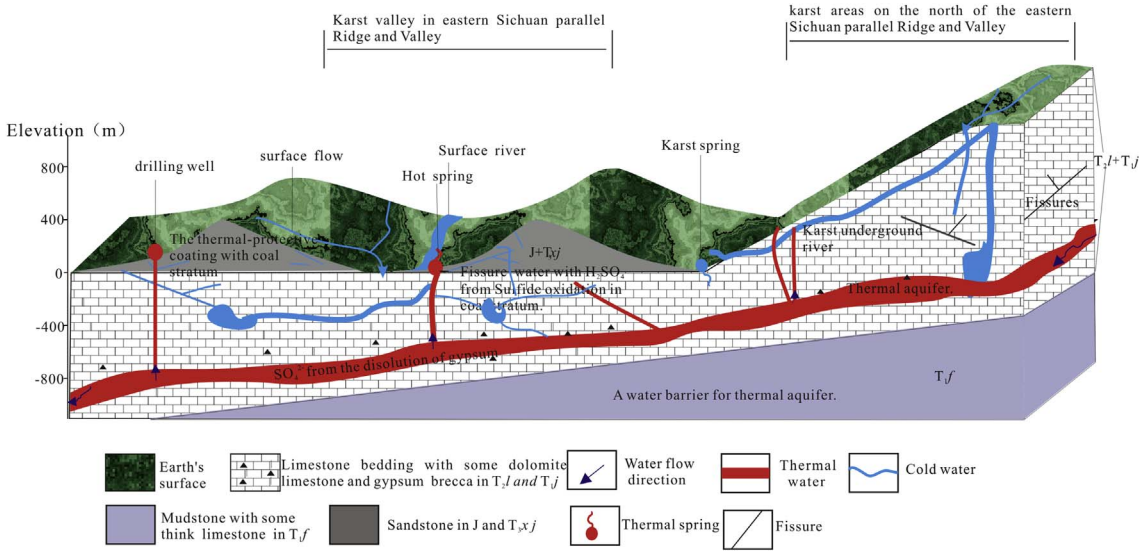


**Fig. 8.** Conceptual model of formation and evolution of the thermal waters in Chongqing area.

carbonic acid and sulfuric acid derived from the oxidation of sulfide minerals in the Upper Triassic Xujiahe Formation.

## 6. Conclusions

The integration of hydrogeochemical and isotopic data can provide key information for deciphering the origin and genesis of the thermal waters. The major chemical compositions of the analyzed thermal waters from Chongqing area was characterized by Ca-$SO_4$ and low alkalinity. The $\delta^2H$ and $\delta^{18}O$ values of the thermal waters ranged from −48.6‰ to −63.1‰ with an average value of −54.2‰, and from −6.5‰ to −9.2‰ with an average value of −8.0‰, respectively, indicating the thermal waters originated from the local rain water with an elevation of 415 m–1453 m above mean sea level. The estimated geothermal temperatures varied from 63.8 °C to 78.3 °C (Quartz), indicating a depth of the geothermal reservoir ranged from 411 m to 1728 m, which is located in the Lower Triassic Jialingjiang formation. The $\delta^{34}S\text{-}SO_4^{2-}$ and $\delta^{18}O\text{-}SO_4^{2-}$ in the geothermal waters ranged from 29.7‰ to 34.1‰ with a mean value of 32.1‰, and from 12.5‰ to 16.5‰ with a mean value of 15.2‰, respectively, suggesting that the high $SO_4^{2-}$ concentrations and $\delta^{34}S\text{-}SO_4^{2-}$ resulted mainly from the dissolution of gypsum in the second part of the Lower Triassic Jialingjiang Formation and partly form the oxidation of sulfide minerals in the Upper Triassic Xujiahe Formation in the study area. Three water-rock interactions in the thermal system were unveiled by the hydrogeochemical and isotopic models, of which 73% (Model 1) and 74% (Model 2), 20% (Model 1) and 21% (Model 2), and 7% (Model 1) and 5% (Model 2) of ($Ca^{2+}+Mg^{2+}$) in the geothermal waters were derived from the gypsum dissolution, carbonate dissolution by carbonic acid, and carbonate weathering by $H_2SO_4$ from the oxidation of sulfide minerals, respectively, and 91.5% (Model 1) and 91.1% (Model 2), and 8.5% (Model 1) and 8.9% (Model 2) of $SO_4^{2-}$ in the geothermal waters were derived from the gypsum dissolution and carbonate weathering by $H_2SO_4$ from the oxidation of sulfide minerals, respectively.

Thus, meteoric water originated from mountain area with high elevation infiltrates through the exposed carbonate karst fissures or conduits to the deep carbonate aquifer with some gypsum which comprises of the geothermal reservoir in Chongqing area. During this processes, the carbonate rocks is weathered by carbonic acid and $H_2SO_4$ from the oxidation of sulfide minerals, and the gypsum is dissolved, and the water is gradually heated and forms finally the thermal waters with high $Ca^{2+}$ and $SO_4^{2-}$ concentrations. And then the thermal waters are exposed in artesian springs from the anticlinal axis or drained in wells.

## Acknowledgement

This research was supported by the national key research and developmental program of China (2016YFC0502306), and the National Natural Science Foundation of China (NSF Grant nos. 41302213 and 41472321), and Guangxi Science Foundation (Grant No. 2013GXNSFBA019221). Special thanks are given to Peng Wang, Min Cao and Yanfang Gao for their help on the fieldwork, and prof. Simon Bottrell (University of Leeds, UK) for many helpful discussions. The authors also appreciate the constructive comments and suggestions by prof. Ian Cartwright, Michael Kersten and two anonymous reviewers.

## Appendix A. Supplementary data

Supplementary data related to this article can be found at http://dx.doi.org/10.1016/j.apgeochem.2017.11.011.

## References

Berge, T.B., Veal, S.L., 2005. Structure of the Alpine formland. Tectonics 24 TC 5011.
Boschetti, T., Venturelli, G., Toscani, L., Barbieri, M., Mucchino, C., 2005. The Bagni di Lucca thermal waters (Tuscany, Italy): an example of Ca-$SO_4$ waters with high Na/Cl and low Ca/$SO_4$ ratios. J. Hydrol. 307, 270–293.
Bottrell, S.H., Moncaster, S.J., Tellam, J.H., Lloyd, J.W., Fisher, Q.J., Newton, R.J., 2000. Controls on bacterial sulphate reduction in a dual porosity aquifer system: the Lincolnshire Limestone aquifer. Engl. Chem. Geol. 169, 461–470.
Bottrell, S.H., Newton, R.J., 2006. Reconstruction of changes in global sulfur cycling from marine sulfate isotopes. Earth-Sci. Rev. 75, 59–83.
Capecchiacci, F., Tassi, F., Vaselli, O., Bicocchi, G., Cabassi, J., Giannini, L., Nisi, B., Chiocciora, G., 2015. A combined geochemical and isotopic study of the fluids discharged from the Montecatini thermal system (NW Tuscany, Italy). Appl. Geochem 59, 33–46.
Cao, Y., 2007. Study on Geochemical Characteristies of Warm Spring Water and Travertine in North Springs of Chongqing. Master Thesis. Southwest University (In Chinese with English abstract).
Çelmen, O., 2008. Hydrogeochemical and Isotopic Investigation of the Thermal and Mineralized Springs between Sivrihisar and Beypazarı Region (In Turkish). PhD Thesis. Ankara University, Graduate School of Natural and Applied Sciences, Ankara, pp. 239.
Çelmen, O., Çelik, M., 2009. Hydrochemistry and environmental isotope study of the geothermal water around Beypazarı granitoids, Ankara. Turk. Environ. Geol. 58 (8), 1689–1701.
Chandrajith, R., Barth, J.A.C., Subasinghe, N.D., Merten, D., Dissanayake, C.B., 2013. Geochemical and isotope characterization of geothermal spring waters in Sri Lanka: evidence for steeper than expected geothermal gradients. J. Hydrol. 476, 360–369.
Clark, K.I., Fritz, P., 1997. Environmental Isotopes in Hydrogeology. Lewis Publishers, New York, pp. 328.
Clarke, W.B., Thode, H.G., 1964. The isotopic composition of krypton in meteorites. J. Geophys. Res. 69 (17), 3673–3679.
Claypool, G.E., Holser, W.T., Kaplan, I.R., Sakai, H., Zak, I., 1980. The age curves of sulfur and oxygen isotopes in marine sulfate and their mutual interpretation. Chem. Geol.

28, 199–260.
Dublyansky, Y.V., 1995. Speleogenetic history of the Hungarian hydrothermal karst. Environ. Geol. 25, 24–35.
Dupalová, T., Sracek, O., Vencelides, Z., Žák, K., 2012. The origin of thermal waters in the northeastern part of the Eger Rift. Czech Repub. Appl. Geochem 27, 689–702.
Fatma, G., Esra, H., Arzu, F.E., 2011. Hydrogeochemistry, environmental isotopes and the origin of the Hamamayagi Ladik thermal spring (Samsun, Turkey). Environ. Earth Sci. 62 (7), 1351–1360.
Fournier, R.O., Rowe, J.J., 1966. Estimation of underground temperatures from the silica content of water from hot springs and wet-steam wells. Am. J. Sci. 264, 685–697.
Fournier, R.O., 1977. Chemical geothermometers and mixing models for geothermal system. Geothermics 5, 41–50.
Gao, C.X., Shao, L.Y., Li, C.N., 2009. Sequence stratigraphy and coal accumulation of the upper Triassic Xujiahe Formation in eastern Sichuan basin. J. Palaeogeogra 11 (6), 689–697 (In Chinese with English abstract).
González, E.P., Birkle, P., Torres-Alvarado, I., 2000. Evolution of the hydrothermal system at the geothermal field of Los Azufres, Mexico, based on fluid inclusion, isotopic and petrologic data. J. Volcanol. Geotherm. Res. 104, 277–296.
Gunn, J., Bottrell, S.H., Lowe, D.J., Worthington, S.R.H., 2006. Deep groundwater flow and geochemical processes in limestone aquifers: evidence from thermal waters in Derbyshire, England, UK. Hydrogeol. J. 14, 868–881.
Hong, Y.T., Zhang, H.B., Zhu, Y.X., Piao, H.C., Jiang, H.B., Ceng, Y.J., Liu, A.S., 1992. Sulfur isotopic compositions of coal and Sulfur isotope fractionation during coal combustion in China. Chin. Sci. Chem. 22 (8), 868–873 (In Chinese with English abstract).
Hong, Y.T., Zhang, H.B., Zhu, Y.X., Piao, H.C., Jiang, H.B., Liu, D.P., 1994. Sulfur isotopic composition of precipitation in China. Adv. Nat. Sci. 4 (6), 741–745.
Jennifer, L., Lewicki, T.F., Williams, S.N., 2000. Chemical and isotopic compositions of fluids at Cumbal Volcano, Colombia: evidence for magmatic contribution. Bull. Volcanol. 62 (4–5), 347–361.
Juske, H., Kazimierz, R., Shabtai, C., 2008. Isotope effects in the evaporation of water: a status report of the Craig-Gordon model. Isot. Environ. Healt. S. 44 (1), 23–49.
Kah, L.C., Lyons, T.W., Chesley, J.T., 2001. Geochemistry of a 1.2 Ga carbonate-evaporite succession, northern Baffin and Bylot Islands: implications for Mesoproterozoic marine evolution. Precambrian Res. 111 (1–4), 203–234.
Kah, L.C., Lyons, T.W., Frank, T.D., 2004. Low marine sulphate and protracted oxygenation of the Proterozoic biosphere. Nature 431 (7010), 834–838.
Keller, B., 1991. Hydrology of the Swiss Molasse Basin: a review of current knowledge and considerations for the future. Eclogae Geol. Helv. 85 (3), 611–652.
Kusakabe, M., Komoda, Y., Takano, B., Abiko, T., 2000. Sulfur isotopic effects in the disproportionation reaction of sulfur dioxide in hydrothermal fluids: implications for the $\delta^{34}S$ variations of dissolved bisulfate and elemental sulfur from active crater lakes. J. Volcanol. Geotherm. Res. 97 (1–4), 287–307.
Krouse, H.R., Mayer, B., 2000. Sulfur and oxygen isotopes. In: cook, P., Herczey, A.L. (Eds.), Envirnmental Tracers in Subsurface of Hydrology. Kluwer Academic Publishers Nonwell, Massachusetts, pp. 195–232.
Li, T.Y., Li, H.C., Shen, C.Z., Yang, C.X., Li, J.Y., Yi, C.C., Yuan, D.X., Wang, J.L., Xie, S.Y., 2010. Study on the δD and $\delta^{18}O$ characteristics of meteoric precipitation during 2006-2008 in Chongqing, China. Adv. Water Sci. 21 (6), 757–765 (In Chinese with English abstract).
Li, X.D., Liu, C.Q., Liu, X.L., Bao, L.R., 2011. Identification of dissolved sulfate sources and the role of sulfuric acid in carbonate weathering using dual-isotopic data from the Jialing River, Southwest China. J. Asian Earth Sci. 42 (3), 370–380.
Li, X.Q., Bao, H.M., Gan, Y.Q., Zhou, A.G., Liu, Y.D., 2013. Multipie oxygen and sulfur isotope compositions of secondary atmospheric sulfate in a megacity in central China. Atmos. Environ. 81 (4), 591–599.
Lin, Y.T., Gao, L.M., Song, H.B., 1998. Sulfur isotopic composition of the marine Triassic in the Sichuan basin and its geological significance. Geology-Geochem 26 (4), 43–49 (In Chinese with English abstract).
Liu, B.Y., 2005. Chongqing is a spa underground ocean - an area of about 10,000 square kilometers. Sci. Advis. 23 (12), 47 in Chinese.
Loges, A., Wagner, T., Kirnbauer, T., Susanne, G.S., Bau, M., Berner, Z., Gregor, M.G., 2012. Source and origin of active and fossil thermal spring systems, northern Upper Rhine Graben. Ger. Appl. Geochem 27, 1153–1169.
Martinez, S.R., 1993. Caractérisation minéralogique, géochimique et isotopique du champ géothermique de Los Humeros, Mexique. Thèse DoctoratINPL-CNRS, Nancy, France 233pp.
McDermott, J.M., Shuhei, O.S., Tivey, M.K., Jeffrey, S., Seewald, J.S., Wayne, C., Shanks III, W.C., Solow, A.R., 2015. Identification of sulfur sources and isotopic equilibria in submarine hot-springs using multiple sulfur isotopes. Geochim. Cosmochim. Acta 160, 169–187.
Nanjiang Hydrogeological & Engineering Geology Brigade, Geology and Mineral Resources Bureau of Investigation, Sichuan province, China. 1977. 1:20 000 regional hydrogeological investigation reports People's Republic of China (Chongqing pieces). 1977.
Ohmoto, H., 1986. Stable isotope geochemistry of ore deposits. Rev. Mineral. 16, 491–560.
Orti, F., Gündoğan, İ., Helvac, C., 2002. Sodium sulphate deposits of Neogene age: the Kirmir formation, Beypazarı basin. Turk. Sediment. Geol. 146, 305–333.
Palmer, M.R., Helvac, C., Fallick, A.E., 2004. Sulphur, sulphate oxygen and strontium isotope composition of Cenozoic Turkish evaporites. Chem. Geol. 209, 341–356.
Peters, M., Strauss, H., Petersen, S., Kummer, N.A., homazo, C., 2011. Hydrothermalism in the Tyrrhenian Sea: inorganic and microbial sulfur cycling as revealed by geochemical and multiple sulfur isotope data. Chem. Geol. 280 (1–2), 217–231.
Phillips, D.L., Gregg, J.W., 2001. Uncertainty in source partitioning using stable isotopes. Oecologia 127, 171–179.
Philips, D.L., Koch, P.L., 2002. Incorporating concentration dependence in stable isotope mixing models. Oecologia 136, 261–269.
Rye, R.O., Back, W., Hanshaw, B.B., Rightmire, C.T., Pearson, F.J., 1981. The origin and isotopic composition of dissolved sulfide in groundwater from carbonate aquifers in Florida and Texas. Geochim. Cosmochim. Acta 45, 1941–1950.
Risacher, F., Fritz, B., Hauser, A., 2011. Origin of components in Chilean thermal waters. J. S. Am. Earth Sci. 31 (1), 153–170.
Rissmann, C., Leybourne, M., Benn, C., Christenson, B., 2015. The origin of solutes within the groundwaters of a high Andean aquifer. Chem. Geol. 396, 164–181.
Samborska, K., Halas, S., Bottrell, S.H., 2013. Sources and impact of sulphate on groundwaters of Triassic carbonate aquifers, Upper Silesia. Pol. J. Hydrol. 486, 136–150.
Sichuan Geological Bureau, 1991. Sichuan Geology. Geological Publishing House, Beijing, China, pp. 206–242.
Spence, M.J., Bottrell, S.H., Thornton, S.F., Lerner, D.N., 2001. Isotopic modelling of the significance of sulphate reduction for phenol attenuation in a polluted aquifer. J. Contam. Hydrol. 53, 285–304.
Szynkiewicz, A., Borrok, D.M., Skrzypek, G., Rearick, M.S., 2015. Isotopic studies of the Upper and Middle Rio Grande. Part 1-Importance of sulfide weathering in the riverine sulfate budget. Chem. Geol. 411, 323–335.
Wang, H.C., 1991. Introduction of Isotopic Hydrogeology. In: Chinese. Geological Publishing House, Beijing, China, pp. 156–157.
Yang, P.H., Cheng, C., Xie, S.Y., et al., 2017. Hydrogrochemistry and geothermometry of deep thermal water in the carbonate formation in the main urban area of Chongqing, China. J. Hydrol. 549, 50–61.
Yu, J.S., Zhang, H.B., Yu, F.J., Liu, D.P., 1980. Oxygen isotopic composition of meteoric water in the eastern part of Tibet. Geochemica 2, 113–121 (In Chinese with English abstract).
Zhou, D., Ju, Y.W., Li, J.Q., 1954. Qualitative Analysis (Volume III). Higher Education Press, Beijing, China, pp. 715 (In Chinese).